

**Rogue waves in mode-locked fiber lasers**Alexandr Zaviyalov,<sup>\*</sup> Oleg Egorov, Rumen Iliev, and Falk Lederer*Institute of Condensed Matter Theory and Solid State Optics, Friedrich-Schiller-Universität Jena, Max-Wien-Platz 1,  
D-07743 Jena, Germany*

(Received 1 April 2011; published 23 January 2012)

We report on the theoretical observation of optical rogue waves in a dissipative system, namely, a mode-locked fiber laser. These rogue waves are pulses of huge peak power which may chaotically appear in the laser. They exist in the normal dispersion regime and exhibit peak powers exceeding those of stable dissipative solitons by a factor of 13. Their height exceeds the so-called significant wave height by a factor of 6. The peak power of the rogue waves can be changed by varying the laser gain. These rogue waves arise from noise by a peculiar nonlinear focusing process of the intracavity light in this dissipative system without requiring any specific initial conditions. Moreover, we identify the crucial effect of gain saturation on the focusing process and, consequently, on the peak amplitude of rogue waves. Similar to rogue events in the ocean, the laser rogue pulses are also accompanied by holes which are moving dark solitons.

DOI: [10.1103/PhysRevA.85.013828](https://doi.org/10.1103/PhysRevA.85.013828)

PACS number(s): 42.65.Tg, 42.55.Wd, 42.65.Sf

**I. INTRODUCTION**

Suddenly appearing walls of water or so-called rogue waves (RWs) are devastating phenomena on the ocean which are responsible for many sunken ships and lost human lives. They appear from nowhere, are short-lived, and are extremely rare. RW phenomena are still poorly investigated because their systematic study is extremely difficult in the real environment due to the high risk and their unpredictable (random) appearance on the ocean surface. Neither the conditions for their generation nor the very formation process are sufficiently well understood. The definition of RWs is not very sharp and was introduced based on the description of this phenomenon on the ocean [1,2]. Huge wave events are termed RWs, first, if they have a peak amplitude exceeding the significant wave height (the average wave height of the largest one-third of the waves) by 2–2.5 times or more; second, if their appearance (and disappearance) is random and unpredictable; and third, if they occur more frequently than Gaussian statistics predicts. In this paper we also use this RW definition.

Possible mechanisms of RW formation have been described in the framework of the stochastic, linear, and nonlinear theories [2]. Results obtained from the stochastic theory based on the Rayleigh distribution show that an RW with an amplitude 3 times higher than the significant wave height can appear upon a storm lasting 21 years, which contradicts the actual observations [2,3].

In the framework of the linear theory, the RW phenomenon can be explained as spatiotemporal or spatial focusing due to different group velocities of the different wave components in a dispersive and/or diffractive medium [4,5]. Also, more complicated formation mechanisms have been discussed, accounting for atmospheric forcing (pressure, wind flow) [6–8] or extreme currents (e.g., the Gulf Stream) which cause an anisotropic dispersion relation [9,10].

To date the nonlinear approach relies on solutions of the nonlinear Schrödinger equation (NLSE) which describes, in the first order, the dynamics of deep-water waves [17]. Various

possible mechanisms of RW formation have been discussed. The first relies on the excitation of breather solutions in a modulationally unstable system such as algebraic (Peregrine solitons) [11], time periodic (Ma solitons) [12], and spatially periodic breathers (Akhmediev breathers) [13,14], respectively. A further nonlinear formation mechanism compares to the linear one but additionally takes into account amplitude-dependent effects [2,15]. As a possible scenario of RW formation the collision between two or more solitons has also been discussed, where the amplitude enhancement can be very significant (factor of 4 or even more) [16].

It was only natural to search for optical RW events because pulse propagation in optical fibers may likewise be described by NLSEs or their generalizations if effects beyond second-order linear dispersion and nonlinear self-phase modulation are taken into account. Thus it might be expected that interesting huge-amplitude phenomena, which might find various applications, can be observed. But there is another, potentially more important aspect. The optical environment could represent a convenient laboratory for systematically studying and understanding RW phenomena such as their generation and evolution. There are different claims for having theoretically and experimentally observed rogue events in conservative (systems without loss and gain) fiber optical systems. In particular, a series of works was devoted to the formation of optical rogue solitons upon supercontinuum generation in fibers, based on the collisions with other solitons [19–23]. Another kind of optical RWs in passive fibers are breathers, which were obtained analytically as solutions to the NLSE but require specific initial conditions to be excited [23–25]. In addition to these passive systems, RWs have also been obtained in optical systems with gain. Such RW-like extreme value fluctuations were investigated in fiber Raman amplifiers where a partially incoherent pump was used [26]. Spatiotemporal RWs were reported by Montina *et al.* in a liquid crystal light valve optical oscillator [27]. In this case their generation was caused by a nonlocal spatial coupling of the cavity field.

Similarly to the situation on the ocean, where the wind represents an external pump during RW formation [18], in

<sup>\*</sup>aleksandr.zaviyalov@uni-jena.de

fiber lasers this pump mechanism is provided by the gain medium. Hence, due to these analogies, here we propose a mode-locked fiber laser as a perfect optical test bed for the investigation of RW phenomena which takes into account such significant effects as dispersion (analog to diffraction), Kerr nonlinearity, external pumping, and linear and nonlinear dissipation. Furthermore, optical RWs in fiber lasers can be investigated systematically under definite and safe conditions.

In this article, we numerically demonstrate the formation of optical RWs (temporal pulses) in mode-locked fiber lasers. We show that these pulses have a huge peak power. They appear chaotically in the laser cavity and disappear without any trace. In agreement with the calculated statistical distribution, their strength (amplitude in oceanology, but peak power in fiber optics) can be as much as 6 times greater than the significant wave height (the average peak power of the highest one-third of the waves) and exceed by more than 13 times the maximum possible peak power of the stable soliton in this laser. The appearance of these giant pulses is a fairly rare event, but at the same time, its probability is much higher than Gaussian statistics predicts. Hence, based on the above-introduced definition they can be termed RWs and their formation in the laser cavity can be characterized as a peculiar focusing process which is of a nonlinear dissipative nature and does not require any specific initial conditions. It differs fundamentally from those nonlinear processes previously discussed such as multisoliton collisions, nonlinear focusing and breather excitation. Moreover, optical RWs exist in the normal dispersion regime where classical bright solitons do not exist for focusing fiber Kerr nonlinearity.

The paper is organized as follows. In Sec. II we consider the probability density function of the laser output signal for three simple cases: a stable single pulse, a periodically appearing and then disappearing single pulse, and two periodically appearing pulses of different amplitudes. These examples are helpful for interpretation of the results. In Sec. III we briefly present the equations used for modeling the fiber ring laser in the lumped approach, where all individual elements in the cavity are modeled by separate equations and the pulses are sequentially propagated. Section IV is devoted to the numerical results, which demonstrate the chaotic appearance of RWs in a mode-locked fiber laser. This operation regime is obtained by a smooth transition from the region of stable dissipative soliton generation. Finally, we summarize our work in Sec. V.

## II. STATISTICAL DESCRIPTION

Since one of the major RW features is their random appearance, the probability density function of the wave peak power is the most appropriate measure of this phenomenon. For a  $(1 + 1)$ -dimensional problem, e.g., pulses in a laser, the probability distribution can be defined and calculated in a different manner. In the present article we use the most accurate one, in which the statistics displays the frequency of occurrence of pulses (the events) as a function of their peak power. For this purpose, all pulses of the randomly recorded output have to be counted (not just the biggest one). In doing so over many round-trips, the respective probability distribution can be obtained. This definition is quite intuitive and can be

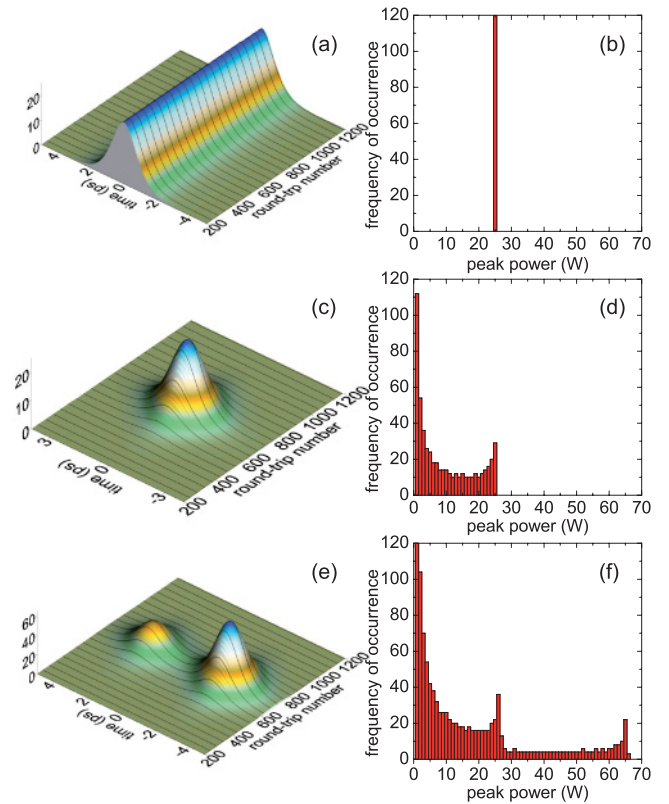


FIG. 1. (Color online) Examples of the calculated statistical distribution for different sech-shape pulses. (a) Constant-amplitude pulse; (c) single arising and vanishing pulse; (e) two arising and vanishing pulses of different amplitudes; (b, d, f) the respective calculated statistics.

easily realized in experiments but yields some nontrivial results as demonstrated in the following simple example.

Figure 1 shows typical output signals as a function of the round-trip number as well as the corresponding calculated probability distribution. For the sake of simplicity, we manually construct the laser output by periodic (along the round-trip axis) functions where only a single period is shown. As expected, the well-known stable single-pulse generation in the laser causes a  $\delta$ -like statistical distribution, because every output contains only a single pulse with invariant amplitude. But the statistical picture differs dramatically when a pulse arises and then vanishes [see Fig. 1(b)]. Since the output signal contains a pulse with varying peak amplitude, dependent on the round-trip number, the statistics includes pulses with different peak powers, finally leading to an L-shaped probability density function. The probability function has two local maxima, corresponding to the two “turning points” of the largest and vanishing peak power, respectively. The maxima appear because in these regions of extreme amplitudes, the first derivative (along the round-trip axis) is close to 0, and consequently, pulses with such amplitudes occur more frequently. If the transition from increasing to decreasing peak power is instantaneous, i.e., the envelope along the round-trip axis has a conical form with a central kink, the second maximum in the probability distribution disappears. Although the present probability distribution is L-shaped, it does not represent a rogue event because the

peak power of neither pulse exceeds the significant wave height by at least 2 times. This example emphasizes that the L-shaped probability density profile is only a necessary, and not a sufficient, condition for RW events.

As required [22], the probability distribution calculated as shown correctly takes into account all peak amplitudes independently of their magnitude and position. The third example clarifies that two arising and then vanishing pulses of different amplitudes are properly expressed in the statistical distribution as the superposition of two L-shaped profiles, and vice versa; from Fig. 1(f) we can easily extract that the output signal contains two pulses of different amplitudes, which appear and disappear.

### III. LASER MODEL

For numerical modeling we use a simple scheme of a fiber ring laser which consists of a doped fiber, a saturable absorber, and an output coupler. Our simulations are based on the lumped approach, where each element is treated separately. The doped fiber is described by a modified NLSE, where it has been assumed that the carrier optical frequency equals the dopant's atomic resonance frequency [28],

$$\begin{aligned} \frac{\partial U(z,t)}{\partial z} + \frac{i}{2}(\beta_2 + ig(z)T_1^2) \frac{\partial^2 U(z,t)}{\partial t^2} \\ = \frac{g(z)U(z,t)}{2} + i\gamma|U(z,t)|^2U(z,t), \end{aligned} \quad (1)$$

where  $U(z,t)$  is the envelope of the pulse,  $z$  is the propagation coordinate,  $t$  is the retarded time,  $\beta_2$  is the group velocity dispersion, and  $\gamma$  represents the fiber nonlinearity.  $g(z)$  is the saturable gain of the doped fiber, and  $T_1$  the dipole relaxation time (inverse gain line width in parabolic approximation). Assuming that the conditions are close to stationary, the gain can be approximated by Ref. [29]

$$g(z) = \frac{g_0}{1 + \int_{\text{pulses}} |U(z,t)|^2 dt / E_{\text{sat}}^{\text{Gain}}}, \quad (2)$$

where  $g_0$  is the small-signal gain, which characterizes the pump level, and  $E_{\text{sat}}^{\text{Gain}}$  is the gain saturation energy. To describe the saturable absorber, we use the well-known transmission equation in the instantaneous response approximation [29],

$$U_{\text{out}}(t) = U_{\text{in}}(t) \exp\left(-\frac{1}{2} \frac{\delta_0 \Delta z}{1 + |U_{\text{in}}(t)|^2 / P_{\text{sat}}}\right), \quad (3)$$

where  $\delta_0 \Delta z$  defines the modulation depth of the absorber and  $P_{\text{sat}}$  is the saturation power. For numerical modeling we use the following parameters. The modulation depth of the absorber is 5% and the saturation power  $P_{\text{sat}} = 0.03$  W. The output loss amounts to 30%. For the doped fiber we assume  $L_f = 1$  m, with a positive group velocity dispersion of  $0.01 \text{ ps}^2 \text{ m}^{-1}$ ,  $\gamma = 0.005 \text{ W}^{-1} \text{ m}^{-1}$ ,  $T_1 = 100$  fs,  $g_0 = 0.6 \text{ m}^{-1}$ , and  $E_{\text{sat}}^{\text{Gain}} = 0.1$  nJ. Since for this range of parameters the typical pulse duration is on the picosecond scale, intrapulse Raman effects can be safely neglected [37]. The output signal was always recorded after the output coupler. As the initial condition we use localized, but sufficiently broad noise of a low amplitude. The weak localization of the initial signal is required by the assumption under which Eq. (2) was derived [29]. The localized noise is merely used to demonstrate that pulsing

and rogue events can occur even from almost-arbitrary initial conditions.

### IV. ROGUE WAVE GENERATION

The typical operation regimes of mode-locked fiber lasers have been extensively studied and can also be controlled by changing the small-signal gain in the system. Thus, beginning at small pump levels the laser usually generates stable single dissipative solitons. When the gain is gradually increased the soliton amplitude grows too, until it reaches the limiting value. This limit is well known in laser physics, where a further gain increase leads to pulse breakup [30–32]. Usually this breakup causes the formation of double-pulse (or multipulse) solutions which are known as bound states or soliton molecules [33–36]. In the course of this process the number of pulses in the laser increases with increasing gain, as demonstrated in previous theoretical and experimental works [30–36].

In order to achieve RW generation the laser parameters were chosen such that, for increasing gain, multipulse solutions become unstable or do not exist [33,34]. In this parameter region the laser still shows the typical stable single-pulse behavior for a small gain [see Figs. 2(a) and 2(b)]. But for a larger gain, where the single soliton becomes unstable, the mode-locked fiber laser exhibits a previously unknown behavior. Namely, by gradually increasing the gain, we trace the novel laser dynamics, which corresponds to the operation regime in the transition region between the generation of stable single dissipative solitons and the chaotic generation of rogue pulses with a huge peak amplitude. For example, the laser dynamics is shown in this regime in Figs. 2(c) and 2(d) for  $g_0 = 0.7 \text{ m}^{-1}$ . In this operation regime the chaotic (random) formation of high-power pulses of finite lifetime (about 1000 round-trips) takes place. It is noteworthy that the peak power of these pulses amounts to 22 W (the pulse energy is 66 pJ), while the peak power of the stable dissipative soliton in this laser is limited to 17 W (the soliton energy is about 59 pJ). In other words, this demonstrates that unstable, chaotically appearing pulses can have a larger peak power than stable dissipative solitons in the same system, which is probably a very significant issue for the understanding of RW phenomena.

For further increasing gain the laser dynamics becomes more complicated. In this case, one output signal contains many low-amplitude pulses and sometimes rogue pulses of a huge peak amplitude can suddenly arise and then vanish (see Fig. 3). The rogue pulse peak powers are as large as 70 W (the pulse energy amounts to 109 pJ) for  $g_0 = 1.1 \text{ m}^{-1}$ . For an even bigger gain ( $g_0 = 2.3 \text{ m}^{-1}$ ), the measured peak power amounts to 215 W (the pulse energy is 140 pJ). For the system parameters used, the maximum peak power of a stable dissipative soliton amounts to 17 W (even for a high gain, where some noninteracting separated pulses can coexist). Thus, the peak power of rogue pulses can exceed it by a factor of 13. Since this operation regime provides chaotic pulses, we use the statistical approach for description. In order to provide a truly statistical picture the laser dynamics during 100 000 round-trips was considered and the corresponding statistical distribution was calculated as described above. The respective probability functions are shown in Fig. 4. It can

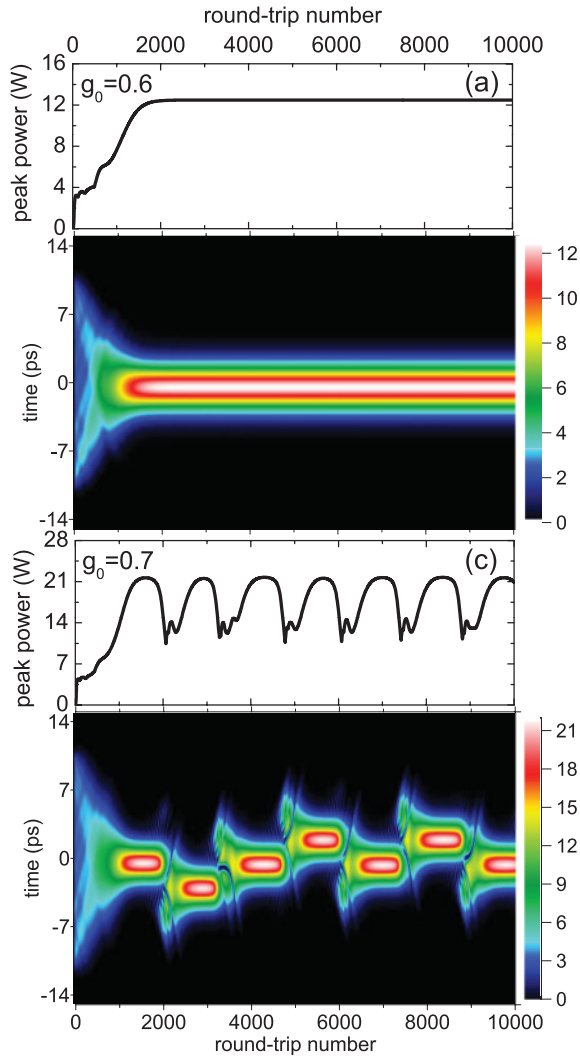


FIG. 2. (Color online) Transition from the well-known dynamics of single dissipative soliton generation ( $g_0 = 0.6 \text{ m}^{-1}$ ) to the novel operation region of chaotically appearing pulses ( $g_0 = 0.7 \text{ m}^{-1}$ ). (a), (c) Peak power and (b), (d) output profile as a function of the round-trip number for  $g_0 = 0.6 \text{ m}^{-1}$  and  $g_0 = 0.7 \text{ m}^{-1}$ , respectively.

be recognized that for  $g_0 = 1.1 \text{ m}^{-1}$  and  $g_0 = 2.3 \text{ m}^{-1}$ , the probability functions are characterized by fat and long tails, which indicate the appearance of huge peak power pulses. It is evident that these pulses generated in a fiber laser with a large gain meet the definition of RWs; namely, they exhibit the required statistical behavior (non-Gaussian behavior with long tails of the probability function) and a huge peak power (bigger than the significant wave height by a factor of 2–2.5 or more), and they appear and disappear spontaneously and unpredictably. First, for rigorous verification we calculated the significant wave height, which amounts to 20 W at  $g_0 = 1.1 \text{ m}^{-1}$  and 36 W at  $g_0 = 2.3 \text{ m}^{-1}$ . Thus the biggest rogue pulses exceed the significant wave height by a factor of 3 or 6 for  $g_0 = 1.1 \text{ m}^{-1}$  and  $g_0 = 2.3 \text{ m}^{-1}$ , respectively. Second, in Fig. 3 the spontaneous appearance and disappearance are shown. Third, the tails of the statistical distributions decay much more slowly than an exponential distribution would predict, which is clearly shown in Fig. 4. Moreover, the

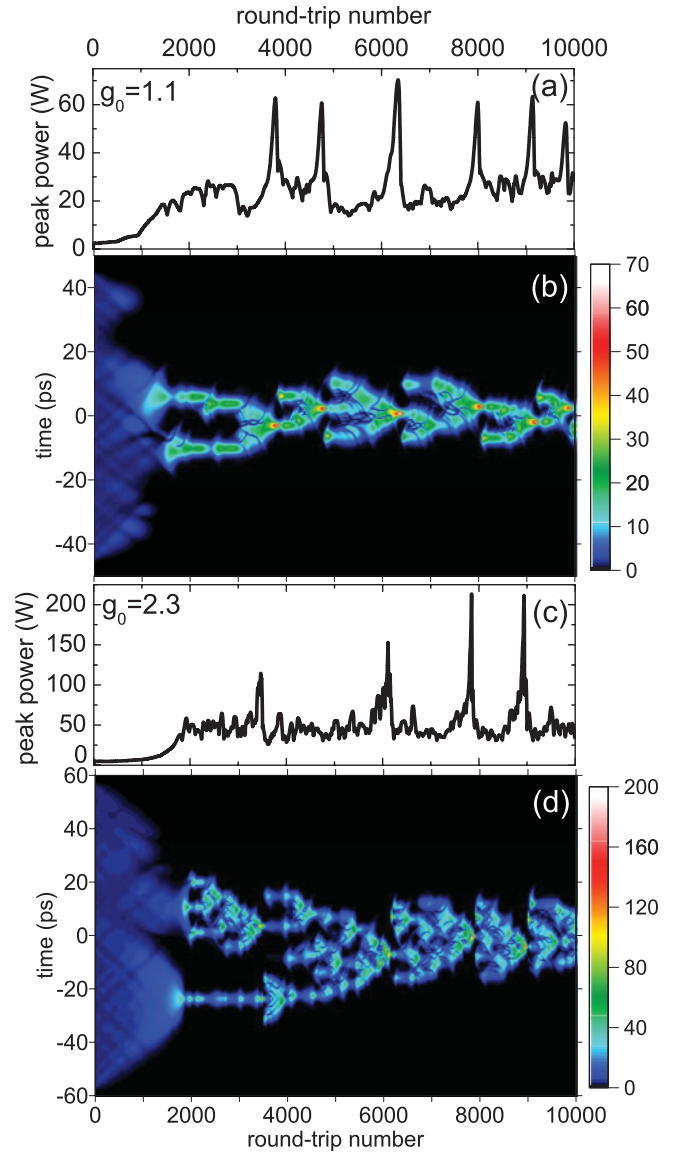


FIG. 3. (Color online) Rogue wave generation in a mode-locked fiber laser initiated from noise. (a), (c) Peak power and (b), (d) output profile as a function of the round-trip number for  $g_0 = 1.1 \text{ m}^{-1}$  and  $g_0 = 2.3 \text{ m}^{-1}$ .

observed RW phenomena in the ocean are accompanied by deep holes which occur before and after the largest crest [2]. Surprisingly, we could also observe these holes in mode-locked lasers (the crossing dark lines in Fig. 3). We could verify that these holes represent moving dark solitons with a characteristic phase jump of  $\sim \pi$  at the hole minima [38,39] (see Fig. 5).

It should be noted that in the transition region where  $g_0 = 0.7 \text{ m}^{-1}$ , the arising pulses are not RWs because the calculated significant wave height amounts to 19.5 W while the biggest detected peak power is only 22 W. Although this peak power is higher than the peak power of stable solitons, they appear more often than exponential statistics would predict and, also, arise spontaneously.

In the operation regime where RWs are generated, two competitive processes can be distinguished (see Fig. 3). On one side the focusing process concentrates almost all

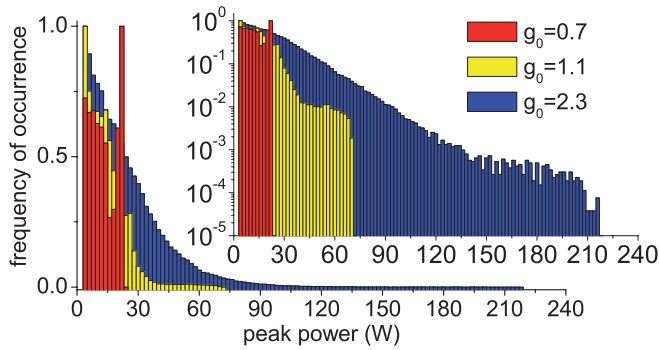


FIG. 4. (Color online) Calculated probability distribution of output pulses as a function of the peak power in linear and logarithmic scales. It is clearly shown that for  $g_0 = 1.1 \text{ m}^{-1}$  and  $g_0 = 2.3 \text{ m}^{-1}$ , the statistics is characterized by long and fat tails, which decay much more slowly than an exponential one.

intra-cavity light at one point that corresponds to the rogue pulse appearance. But simultaneously there is an opposing process which spreads the localized light when the peak power exceeds a certain threshold. Sometimes the diffused light can form a bunch of pulses of relatively low amplitudes which are unstable at such a gain. Finally, the breakup of such a multipulse state leads to a chaotic energy distribution in the cavity, which is again nonlinearly focused. Thus it is a perpetual competition between focusing and diffusing phenomena, with the possible intermediate formation of unstable multipulse states. The most powerful and intense rogue pulses appear in the case where almost all light inside the cavity is focused (see Fig. 3). Hence, the focusing process is the key formation mechanism of optical RWs in the laser.

From Figs. 3 and 6 it can be recognized that the observed focusing phenomenon differs in principle from the well-known classical linear and nonlinear (including intensity dependence) focusing process. Namely, this peculiar focusing starts from random initial conditions in the laser. Furthermore, both

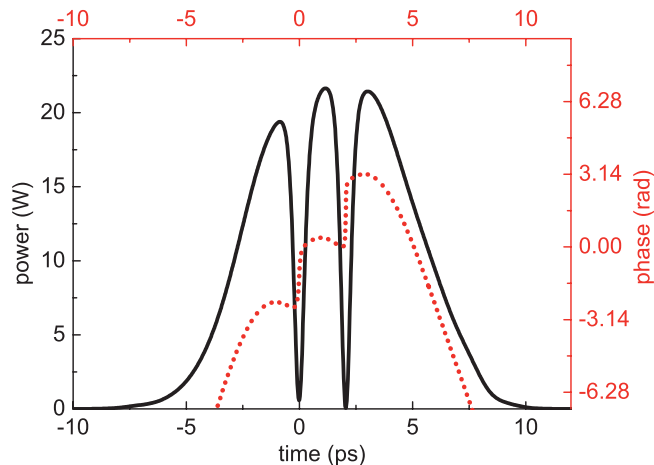


FIG. 5. (Color online) Power [solid (black) line] and phase [dotted (red) line] profiles of holes observed in the output signal taken from Fig. 3(b) after 6000 round-trips;  $g_0 = 1.1 \text{ m}^{-1}$ . Two dark solitons are clearly shown, with the characteristic ( $\sim\pi$ ) phase jump at the power minima.

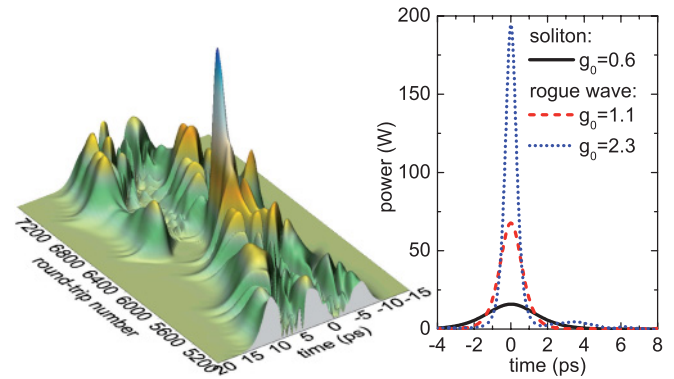


FIG. 6. (Color online) Left: Rogue wave formation process in the mode-locked fiber laser for  $g_0 = 1.1 \text{ m}^{-1}$  [corresponding to Fig. 3(b)]. Right: Profile of the soliton and the two rogue waves obtained with the same laser parameters but a different, small-signal gain.

the observed focusing process and, consequently, the RW formation have a strong nonlinear dissipative nature. In order to demonstrate this we consider RW formation in the laser for varying gain saturation energies, with all other laser parameters kept constant. Since varying the gain saturation energy also entails a change of the effective pump power, the small-signal gain was additionally adjusted. As a benchmark for adjusting the effective gain, the peak amplitude of three noninteracting, isolated pulses was used. Figure 7 shows the statistical distribution of the generated pulses for different values of the gain saturation energy. It is evident that the central portions of the probability functions (peak power up to 35 W) are very similar for both values of  $E_{\text{sat}}^{\text{Gain}}$ . But the appearance of high-amplitude pulses (peak power higher than 35 W) depends significantly on the saturation energy of the gain. For  $E_{\text{sat}}^{\text{Gain}} = 0.1 \text{ nJ}$  the peak power of the generated pulses can be as high as 70 W, while for a higher gain saturation energy, when  $E_{\text{sat}}^{\text{Gain}} = 0.4 \text{ nJ}$  the maximum detected peak power is only 50 W. Thus saturability of the gain has a strong influence on the intracavity focusing process in the mode-locked fiber laser and, consequently, on the RW generation process and peak amplitudes.

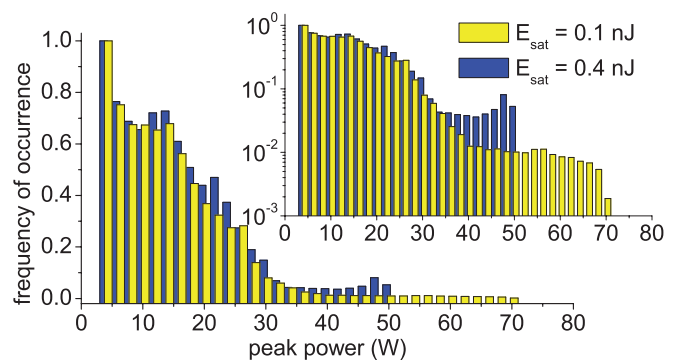


FIG. 7. (Color online) Statistical distribution of the output pulses in a mode-locked laser for the same parameters but different saturation energies of the gain  $E_{\text{sat}}^{\text{Gain}}$ . It can be seen that the gain saturability plays a crucial role in the generation process in the laser, particularly, for the peak amplitudes.

## V. CONCLUSION

In conclusion, we have numerically demonstrated RW generation in a mode-locked fiber laser in a normal dispersion domain. These RWs are pulses of huge peak amplitude which appear chaotically in the laser. The maximum peak amplitude of these rogue pulses can be controlled via the small-signal gain. Thus for  $g_0 = 2.3 \text{ m}^{-1}$  the rogue events can reach a peak power as high as 215 W, which is 13 times larger than the maximum possible peak power of a single stable soliton or a few solitons in this laser and 6 times larger than the significant wave height. For the reduced gain of  $g_0 = 1.1 \text{ m}^{-1}$  the measured peak power of the rogue event amounts to 70 W. The RW formation process was identified to be a peculiar focusing process which is of a nonlinear dissipative nature and can successfully start from random initial conditions. We also identified that nonlinear dissipation, i.e., gain saturability, plays a crucial role in the process of RW generation, in

particular, for their peak amplitudes. Furthermore, similarly to RWs on the ocean, the observed rogue pulses in the laser are accompanied by holes which are moving dark solitons.

The results of this work may be useful for a better understanding of the nature of RWs in the ocean and can also be used as a novel approach for the generation of high-power pulses in laser systems.

During the revision of this paper the related numerical observation of RWs in a fiber laser in an anomalous dispersion domain [40] and the experimental observation of RWs in an optically injected semiconductor laser [41] were published.

## ACKNOWLEDGMENT

Alexandr Zaviyalov acknowledges financial support from the Graduate Research School of Photonics at Friedrich-Schiller-Universität Jena.

- 
- [1] N. Akhmediev and E. Pelinovsky, *Eur. Phys. J. Special Topics* **185**, 1 (2010).
- [2] C. Kharif and E. Pelinovsky, *Eur. J. Mech. B/Fluids* **22**, 603 (2003).
- [3] M. Longuet-Higgins, *J. Marine Res.* **11**, 1245 (1952).
- [4] A. Kurkin and E. Pelinovsky, *Eur. J. Mech. B/Fluid* **21**, 561 (2002).
- [5] E. Pelinovsky, T. Talipova, A. Kurkin, and Ch. Kharif, *Nat. Hazards Earth Syst. Sci.* **1**, 243 (2001).
- [6] J. K. Mallory, *Inst. Hydrog. Rev.* **51**, 99 (1974).
- [7] I. V. Lavrenov, *Mathematical Modeling of the Wind Waves in Spatially Inhomogeneous Ocean* (Hydrometeoizdat, Saint Petersburg, Russia, 1998).
- [8] I. V. Lavrenov, *Nat. Hazards* **17**, 117 (1998).
- [9] D. H. Peregrine, *Adv. Appl. Mech.* **16**, 9 (1976).
- [10] B. S. White and B. Fornberg, *J. Fluid Mech.* **255**, 113 (1998).
- [11] D. H. Peregrine, *J. Austral. Math. Soc. Ser. B* **25**, 16 (1983).
- [12] Y. C. Ma, *Stud. Appl. Math.* **60**, 43 (1979).
- [13] N. Akhmediev and V. I. Korneev, *Theor. Math. Phys.* **69**, 1089 (1986).
- [14] N. Akhmediev, V. M. Eleonskii, and N. E. Kulagin, *Theor. Math. Phys.* **72**, 809 (1987).
- [15] C. Kharif, E. Pelinovsky, T. Talipova, and A. Slunyaev, *JETP Lett.* **73**, 170 (2001).
- [16] P. Peterson, T. Soomere, J. Engelbrecht, and E. van Groesen, *Nonlin. Process. Geophys.* **10**, 503 (2003).
- [17] A. V. Slunyaev, *J. Exp. Theor. Phys.* **101**, 926 (2005).
- [18] C. Kharif and J. Touboul, *Eur. Phys. J. Special Topics* **185**, 159 (2010).
- [19] D. R. Solli, C. Ropers, P. Koonath, and B. Jalali, *Nature* **450**, 1054 (2007).
- [20] G. Genty, C. M. de Sterke, O. Bang, F. Dias, N. Akhmediev, and J. M. Dudley, *Phys. Lett.* **374**, 989 (2010).
- [21] M. Taki, A. Mussot, A. Kuninski, E. Louvergneaux, M. Kolobov, and M. Douay, *Phys. Lett. A* **374**, 691 (2010).
- [22] M. Erkintalo, G. Genty, and J. M. Dudley, *Eur. Phys. J. Special Topics* **185**, 135 (2010).
- [23] J. M. Dudley, G. Genty, F. Dias, B. Kibler, and N. Akhmediev, *Opt. Express* **17**, 21497 (2009).
- [24] N. Akhmediev, J. M. Soto-Crespo, and A. Ankiewicz, *Phys. Lett.* **373**, 2137 (2009).
- [25] N. Akhmediev, J. M. Soto-Crespo, and A. Ankiewicz, *Phys. Rev. A* **80**, 043818 (2009).
- [26] K. Hammani, C. Finot, and G. Millot, *Opt. Lett.* **34**, 1138 (2009).
- [27] A. Montina, U. Bortolozzo, S. Residori, and F. T. Arecchi, *Phys. Rev. Lett.* **103**, 173901 (2009).
- [28] G. P. Agrawal, *Phys. Rev. A* **44**, 7493 (1991).
- [29] A. Zaviyalov, R. Iliew, O. Egorov, and F. Lederer, *J. Opt. Soc. Am. B* **27**, 2313 (2010).
- [30] A. Haboucha, A. Komarov, H. Leblond, F. Sanchez, and G. Martel, *Opt. Fiber Tech.* **14**, 262 (2008).
- [31] B. G. Bale, K. Kieu, J. N. Kutz, and F. Wise, *Opt. Express* **17**, 23137 (2010).
- [32] W. H. Renninger, A. Chong, and F. W. Wise, *J. Opt. Soc. Am. B* **27**, 1978 (2010).
- [33] A. Zavyalov, R. Iliew, O. Egorov, and F. Lederer, *Phys. Rev. A* **79**, 053841 (2009).
- [34] A. Zavyalov, R. Iliew, O. Egorov, and F. Lederer, *Phys. Rev. A* **80**, 043829 (2009).
- [35] A. Zavyalov, R. Iliew, O. Egorov, and F. Lederer, *Opt. Lett.* **34**, 3827 (2009).
- [36] B. Ortaç, A. Zaviyalov, C. Nielsen, O. Egorov, R. Iliew, J. Limpert, F. Lederer, and A. Tünnermann, *Opt. Lett.* **35**, 1578 (2010).
- [37] J. P. Gordon, *Opt. Lett.* **11**, 662 (1986).
- [38] Y. S. Kivshar and B. Luther-Davies, *Phys. Rep.* **298**, 81 (1998).
- [39] H. Zhang, D. Y. Tang, L. M. Zhao, and X. Wu, *Phys. Rev. A* **80**, 045803 (2009).
- [40] J. M. Soto-Crespo, P. Grelu, and N. Akhmediev, *Phys. Rev. E* **84**, 016604 (2011).
- [41] C. Bonatto, M. Feyereisen, S. Barland, M. Giudici, C. Masoller, J. Ríos Leite, and J. Tredicce, *Phys. Rev. Lett.* **107**, 053901 (2011).